Korean J. Chem. Eng., 33(2), 629-637 (2016)
DOI: 10.1007/s11814-015-0161-4

pISSN: 0256-1115
eISSN: 1975-7220

Fabrication of poly(ether sulfone) based mixed matrix membranes modified by TiO_2 nanoparticles for purification of biodiesel produced from waste cooking oils

Farah Sadat Halek*,†, Samaneh Koudzari Farahani*, and Sayed Mohsen Hosseini,†**

*Department of Energy, Materials and Energy Research Center (MERC), Karaj 31787-316, Iran
**Department of Chemical Engineering, Faculty of Engineering, Arak University, Arak 38156-88349, Iran
(*Received 4 February 2015 • accepted 21 July 2015*)

Abstract−Biodiesel produced from waste cooking oils was purified by use of polyethersulfone-co-TiO_2 nanocomposite membranes. The membranes were prepared by solution casting technique through phase inversion method. Titanium dioxide nanoparticles were used as inorganic filler additive in membrane fabricating. The effect of nanoparticle concentration in the casting solution on the physico-chemical characteristics, morphology and performance of prepared membranes was studied. SEM, AFM and XRD analyses were carried out for the characterization of membrane. The results showed uniform nanoparticle distribution in the membranes matrix. XRD results also indicated a crystalline structure for the membranes. Membrane surface roughness was decreased sharply by increase of nanoparticle concentration up to 0.05%wt in membrane matrix and then increased slightly. Membrane flux, rejection, water content, porosity and membrane mechanical strength were enhanced initially by increase of nanoparticles concentration up to 0.05%wt and then decreased by more increase of nanoparticles content ratio. The nanocomposite membrane containing 0.05 wt% TiO_2 showed more appropriate performance compared to others.

Keywords: Nanocomposite Membrane, TiO_2 Nanoparticles, Fabrication/Characterization, Biodiesel Purification, Transesterification

INTRODUCTION

Energy consumption has increased widely due to growth of transportation and industrial sectors. Attention also has been given to looking for alternative fuels. Biodiesel is considered as one of the most promising alternative fuels. It is non-toxic, renewable, biodegradable and safe environmentally compared to petroleum fuels. The emission of carbon monoxide, particulates, unburned hydrocarbons and SO_x is much lower for biodiesel fuel compared to others. Biodiesel is produced from renewable sources such as vegetable oils and animal fats through different techniques such as microemulsion, pyrolysis and transesterification [1-6]. Transesterification is defined as reaction of triglycerides with low molecular weight alcohols such as methanol and ethanol in presence of catalyst (Fig. 1) [1,5,7-13]. Non-purified biodiesel contains impurities such as glycerol, un-reacted methanol, residual catalyst, un-reacted triglyceride and small amounts of soap and water which should be purified necessarily for the improvement of engine performance [2].

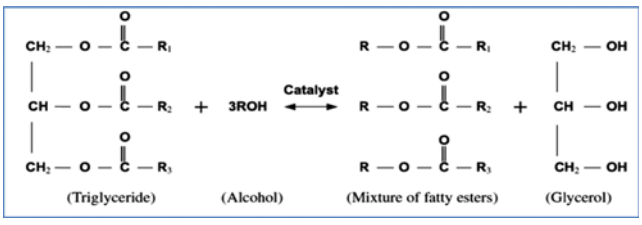

Fig. 1. Transesterification process for biodiesel production.

Different methods have been used for the purification of biodiesel, such as water washing, acid washing, solvents extraction and adsorption. Membrane technology is also well known as new method for biodiesel purification. Energy saving, resource recovery and pollution control are the main reasons for the membrane development and application. Also, it can be easily scaled-up and combined with other processes besides low operating cost [9]. Peyravi et al. [14] prepared nanocomposite solvent resistant PI membranes with different concentration of MWCNTs content ratio via phase inversion method to biodiesel purification. The synthesized membranes showed good behavior in glycerol removal without significant changes in methyl ester flux by using of MWCNTs due to small pore size and high membrane porosity after bulk modification. Gomes et al. [15] used commercial tubular α-Al_2O_3/TiO_2 membranes for biodiesel purification. The influence of ethanol concentration in the feed solution on membrane performance was studied. Low flux and high glycerol rejection were achieved for the feed solution containing 5%wt ethanol. Opposite trend was found for the feed solution containing 20%wt ethanol. Also, results showed that trans-membrane pressure has a significant influence on biodiesel filtration. Alves et al. [4] also used micro and ultrafiltration membranes for biodiesel purification at different trans-membrane pressures and membranes pore sizes. Results revealed that microfiltration membranes were not suitable for the removal of free glycerol from biodiesel. The ultrafiltration membrane with 30 KDa was also not able to pro-

†To whom correspondence should be addressed.
E-mail: Sayedmohsen_Hosseini@yahoo.com, S-Hosseini@araku.ac.ir, F-Halek@merc.ac.ir

duce a purified biodiesel according to the international legislation. Results showed best performance for 10 KDa ultrafiltration membrane compared to others. Saleh et al. [6] designed a membrane system by using ceramic membrane for removal of glycerol from crude FAME. The UF and MF ceramic membranes were used for this aim. The international standards for glycerol content in biodiesel were obtained after 3 h by utilizing of UF membrane at 25 °C. In addition, the smaller pore size of the used UF membrane facilitated glycerol removal compared to the MF membrane.

In other research, Saleh et al. [7] studied performance of ultrafiltration membrane for purification of produced Fatty acid methyl esters (FAME) from canola oil and methanol. The effect of water, soap and methanol in the transesterification reaction on free glycerol separation was studied. A modified polyacrylonitrile (PAN) membrane with 100 KDa molecular weight cut-off was used for the aim. Results showed that low concentrations of water had a considerable effect on glycerol removal from FAME. The optimum concentration of water was found 2.0 g per L of FAME during glycerol removal from biodiesel.

In the current research, PES-co-TiO_2 nanoparticles mixed matrix membranes were prepared by phase inversion method through immersion precipitation technique for separation of dispersed free glycerol from crude biodiesel. Titanium dioxide nanoparticle is one of the well known nanometal oxides that has gained a great deal of attention because of its high hydrophilicity and adsorption capacity, stable chemical property, low cost and safety toward both humans and the environment.

A few researches were found by our literature survey for fabrication of PES membrane modified by TiO_2 nanoparticles for the purification of biodiesel. The biodiesel was produced from waste cooking oils by transesterification method by using of alkaline catalyst. The effects of titanium dioxide nanoparticles concentrations in the casting solution on physico-chemical property, morphology and separation performance of homemade membranes for the purification of biodiesel or glycerol removal were studied.

MATERIALS AND METHOD

1. Materials

Poly ether sulfone (PES Ultrason E6020P with MW=58,000 g/mol) was utilized as membrane base binder. Dimethyl acetamide by Merck was also employed as solvent. Titanium dioxide nanoparticle (TiO_2, nanopowder, anatase crystal, and 15-25 nm particle size) was provided from US Research Nanomaterials, USA. Polyvinyl pyrrolidone (PVP, 25.000 g/mol, Merck) was used as pore former. Methanol (99.9% purity) and sodium hydroxide (NaOH, 98% purity, MW: 39.99) were supplied from Merck Inc. for biodiesel production.

2. Biodiesel Production/Membrane System Feed

Biodiesel was produced from waste cooking oils (restaurant residue, Karaj, Iran) by trans-esterification. The kinematic viscosity and density of used waste cooking oil were measured 46.59 (mm^2/s) and 0.92 (g/mL), respectively. Before trans-esterification reaction, the cooking oil was filtered to remove the residues and precipitates. The oil was heated to 60 °C for 10 min for water removal. The transesterification reaction was in a glass reactor. The reactor contained a thermometer to control the temperature, a reflux condenser to prevent the loss of methanol and a mechanical stirrer for constant agitation. The reactor was also supported by heating mantle to control the temperature around 60 °C. The waste oil was fed into the reactor and preheated before addition of sodium hydroxide (catalyst) and methanol. The molar ratio of methanol to waste cooking oil was adjusted (9 : 1). The reaction time was 2 h and the amount of used catalyst was 1.5%wt. The yield of transesterification reaction was measured 92.5%. The kinematic viscosity, density and pH of produced biodiesel were measured 5.84 (mm^2/s), 0.89 (g/mL) and 7.8, respectively. At the next step, the produced biodiesel was treated with 0.1 N sulfuric acid to naturalize the NaOH and soap. The obtained pH value was measured as 7.8.

The products were then allowed to settle for 8 h. The lower phase (polar glycerol layer) was removed and the upper phase (non-polar layer) was neutralized again by sulfuric acid and used as membrane feed. The glycerol mass percentage in the feed was measured 0.0604 mg glycerol/mg biodiesel.

3. Preparation of Membrane

PES-co-TiO_2 mixed matrix membranes were prepared by phase inversion method through immersion precipitation. The polymeric solution containing PES, DMAC, PVP and TiO_2 nanoparticles was casted on a glass plate by using a casting knife with 200 μm thickness. The prepared films were then immersed in nonsolvent (di-

Table 1. Composition of casting solution for the preparation of home-made membranes

Samples (S_n)	PES (wt%)	PVP (wt%)	DMAC (wt%)	TiO_2 (wt%)
1	16	2	82	0
2	16	2	82	0.02
3	16	2	82	0.05
4	16	2	82	0.1
5	16	2	82	1

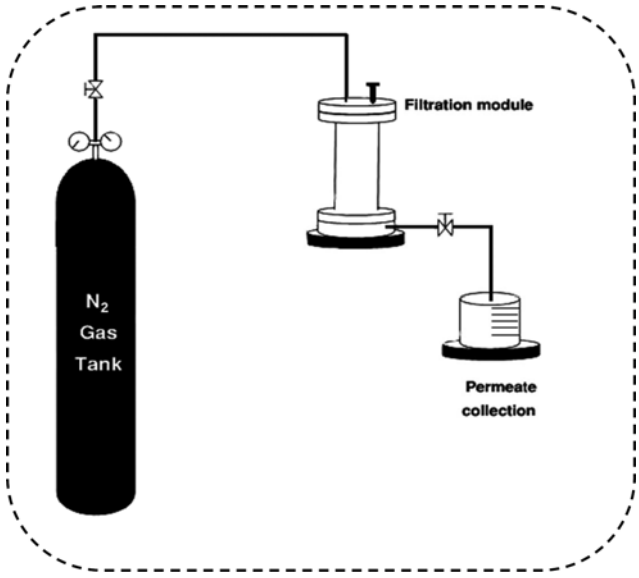

Fig. 2. Schematic diagram of filtration module.

ionized water) bath for precipitation. The immersion process was carried out at ambient temperature. The membranes were washed and stored in distilled water for one day to remove the residual solvent completely. The composition of used casting solution is given in Table 1.

4. Membrane Test Cell

The separation characteristic of prepared membranes was studied by using a dead end cell (Fig. 2). The membranes were located at the end of the cell and fed by produced biodiesel. The fluid passed through the membrane and was collected. The driving force for separation process was provided by nitrogen gas. The applied transmembrane pressure was 2.5 bar.

MEMBRANE CHARACTERIZATION

1. Membrane Flux (J)

A self-made dead end cell was used to measure the flux of prepared membranes. The flux (J) is measured as amount of permeant (ΔV) per unit area of membrane surface area (A) and time (Δt) as follows [16,17]:

$$J = \frac{\Delta V}{A\Delta t}\left(\frac{lit}{m^2 \cdot h}\right) \quad (1)$$

2. Membrane Rejection (R)

The glycerol concentration in feed and permeate was measured

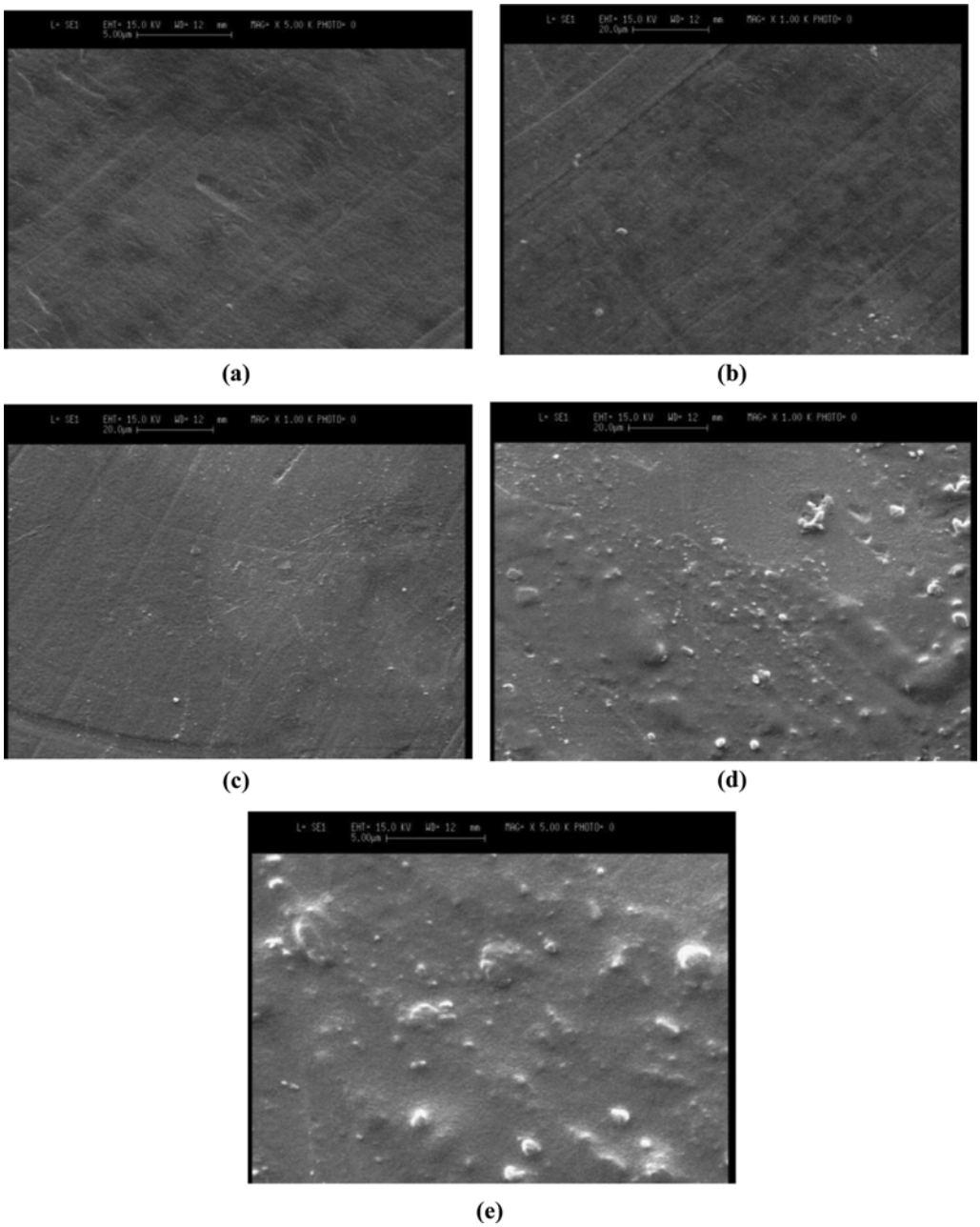

Fig. 3. SEM surface images of prepared membranes with different concentration of TiO_2 nanoparticles: (a) 0 wt%-unmodified ones; (b) 0.02 wt%; (c) 0.05 wt%; (d) 0.1 wt%; (e) 1 wt%.

by UV-Visible instrument. Measurements were according to formation of yellow complex, which is proportional to the amount of free glycerol in the sample. The yellow compound exhibits a maximum absorbance peak at 410 nm. The membrane glycerol rejection is calculated as follows [16-18]:

$$R\% = \left(1 - \frac{C_P}{C_F}\right) \times 100 \quad (2)$$

where (C_F) is glycerol concentration in feed and (C_P) is glycerol concentration in permeate stream.

3. Water Content

The water content of prepared membranes was measured as the weight difference between the dried and swollen membranes. The wet membrane was weighed (OHAUS, Pioneer™, readability: 10^{-4} gr, OHAUS Corp.) and then dried in oven until constant weight was obtained. The water content of membrane was calculated by the following equation [19-23]:

$$\text{water content } \% = \left(\frac{W_{wet} - W_{dry}}{W_{dry}}\right) \times 100 \quad (3)$$

where W_{wet} is the weight of wet membrane and W_{dry} is the weight of dried membrane.

4. Membrane Porosity

Membrane porosity (Pr) was calculated as a function of the membrane weight as follows [24]:

$$P_r = \left(1 - \frac{m}{s \times d \times \rho}\right) \times 100 \quad (4)$$

where m is membrane weight, s is membrane surface area, d is the membrane thickness and ρ is membrane density (ρ=m/v). The membrane volume (V) is obtained from multiplying the membrane surface area by the membrane thickness.

The membrane thickness was measured by a digital caliper device (Electronic outside Micrometer, IP54 model OLR, China).

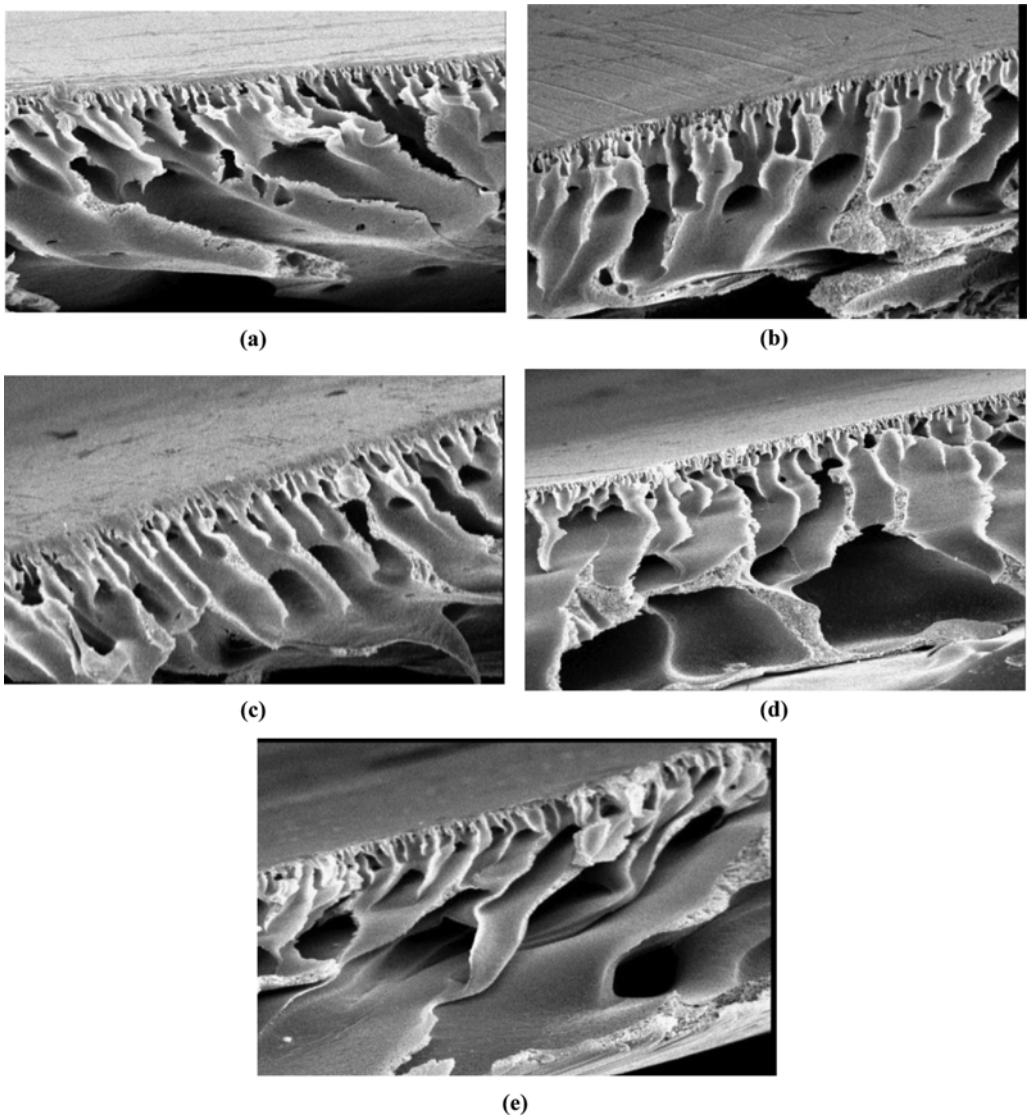

Fig. 4. SEM cross section images of prepared membranes with different concentration of TiO_2 nanoparticles: (a) 0 wt%-unmodified ones; (b) 0.02 wt%; (c) 0.05 wt%; (d) 0.1 wt%; (e) 1 wt%.

5. Scanning Electron Microscope (SEM)

The surface and cross-section of prepared membranes were studied by scanning electron microscope (SEM, Cambridge 360). The membranes were cut into small size pieces. The samples were immersed in liquid nitrogen and were frozen. Then, the samples were broken and kept in air for drying. The dried samples were sputtered by gold for electric conductivity producing.

6. Atomic Force Microscopy (AFM)

The surface roughness of prepared membranes was characterized by atomic force microscopy (AFM, Auto Pro CP, American). The membrane surfaces were imaged in a scan size of 5 μm×5 μm by contact mode.

7. X-ray Diffraction (XRD)

The membranes' structure was studied by X-ray diffraction (XRD, Unisantis XMD300, 45 kV and 0.8 mA, Cu-Kα radiation (1.540510 Å)). XRD diagrams were recorded in the interval $10^o \leq 2\theta \leq 80^o$ at a scan speed of 0.02^o/min.

8. Mechanical Strength

The tensile stress of prepared membranes was investigated by Universal Testing Machine (UTM, SDLATAS, M 350-5 KN, 1 mm/min, at ambient temperature). The samples were cut in to 80 mm× 15 mm pieces. Measurements were made three times for each sample and then their average was reported.

RESULTS AND DISCUSSION

1. Scanning Electron Microscopy (SEM)

The surface and cross-sectional SEM images of prepared membranes are shown in Figs. 3 and 4, respectively. Images showed uniform particle distribution and relatively uniform surfaces for the prepared membranes. Also as seen in SEM images, at high TiO_2 nanoparticle concentration the nanoparticles tended to agglomerate on membrane surface and membrane matrix. Also, SEM images exhibited an asymmetric structure with dense top layer, porous sub-layer and fully developed macro-pores for the prepared membranes. As shown in SEM images, formation of more finger-like pores in membranes sub-layer at 0.05%wt TiO_2 nanoparticles caused to increase membrane porosity. This may be attributed to fast exchange rate between solvent and non-solvent during phase inversion process, which is due to hydrophilic characteristic of TiO_2 nanoparticles [25]. Moreover SEM images showed denser sub-layer with fewer finger-like pores for the mixed matrix membranes containing 0.1 and 1 wt% TiO_2 nanoparticles compared to others. This may be due to increase of casting solution viscosity at high nanoparticles concentration, which reduces the exchange rate between solvent and non-solvent during phase inversion process [26,27].

2. X-ray Diffraction (XRD)

The XRD patterns for the neat PES membrane and PES-co-TiO_2 mixed matrix nanocomposite membrane are shown in Fig. 5. Obtained results show that the structure of PES membrane was changed obviously by using TiO_2 nanoparticles in the casting solution. As shown in this figure, a peak appears at 24.9^o for PES/TiO_2 mixed matrix membranes which is assigned to used TiO_2 NPs. The TiO_2 nanoparticles have nearly peaks at (2θ) 25.3^o, 37.8^o, 48.04^o and 54.38^o [27-31]. The slight movement of peak dispersions illustrates that interaction has occurred between polymer and TiO_2 nanoparticle

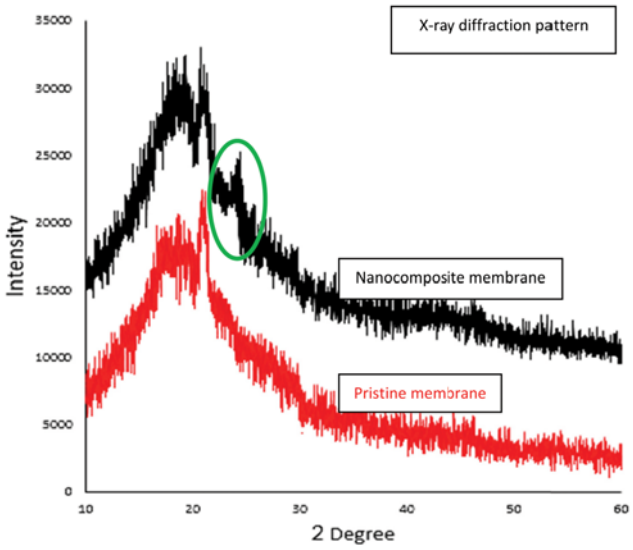

Fig. 5. X-ray diffraction patterns of pristine membrane and mixed matrix ones containing TiO_2 nanoparticles.

[29], which improves the membrane uniformity.

3. Atomic Force Microscopy (AFM)

The surface roughness of prepared membranes was examined by Atomic force microscopy (AFM). Dark and bright areas in AFM images (Fig. 6) refer to valleys and peaks, respectively. AFM results showed that membrane roughness was decreased by utilizing of TiO_2 nanoparticles in membrane matrix. Membrane with low roughness has more antifouling ability [32].

The calculated roughness parameters for the prepared membranes are given in Table 2. Results indicated that membrane roughness decreased sharply from 21.37 to 6.82 nm by increase of TiO_2 nanoparticle concentration up to 0.05 wt% in the casting solution. This happening can be explained with respect to voids and cavities filling by the nanoparticles on membrane surface, which decreases the roughness [30].

The membrane roughness increased slightly from 6.82 to 11.04 nm again by more increase in nanoparticle content ratio from 0.05 to 1 wt%. This may be attributed to nanoparticle agglomeration at high NPs concentration, which increases the roughness of membrane [33,34].

4. Water Content and Porosity

Obtained results (Fig. 7) revealed that increase of TiO_2 nanoparticle concentration in the casting solution up to 0.5%wt led to increase of membrane water content and membrane porosity sharply. This may be attributed to increase of exchange rate between solvent and non-solvent during phase inversion process due to hydrophilic characteristic of TiO_2 nanoparticles, which leads to formation of more finger-like pores in membranes sub-layer. This improves the overall porosity of prepared membranes. Moreover, increase of membrane heterogeneity by utilizing of TiO_2 NPs in the casting solution caused formation of more free spaces in membrane matrix. This results in more water accommodation. The membrane water content and membrane porosity were decreased slightly by further increase of nanoparticle concentration from 0.05 to 1%wt in prepared membranes. This is due to decrease of exchange rate between

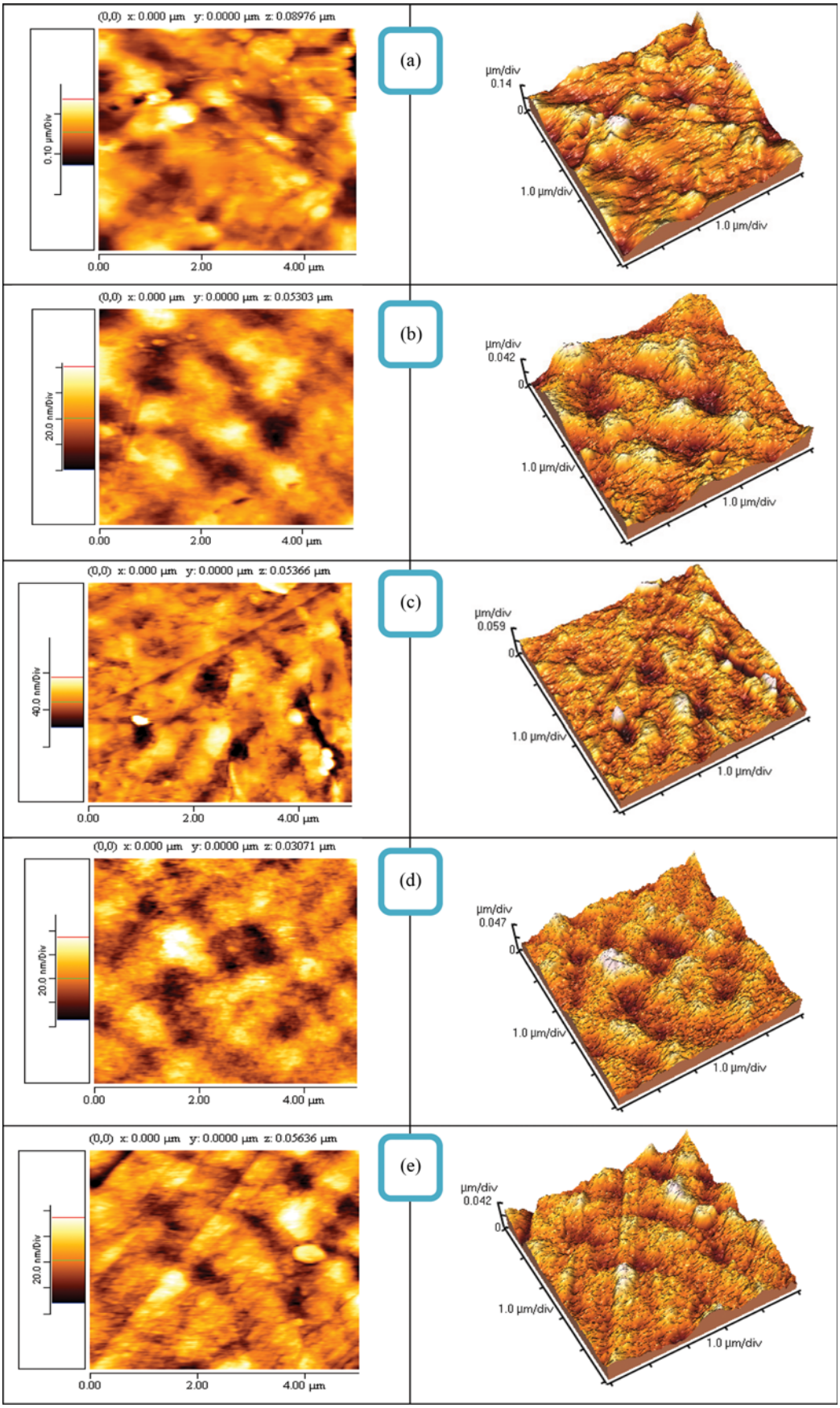

Fig. 6. AFM analysis of prepared membranes with different NPs concentration: (a) 0 wt%, (b) 0.02 wt%, (c) 0.05 wt%, (d) 0.1 wt%, (e) 1%wt.

Table 2. The calculated parameter of surface roughness for the prepared membranes

TiO_2 concentration (wt%)	Average roughness (nm)
0	21.37
0.02	11.52
0.05	6.82
0.1	9.26
1	11.04

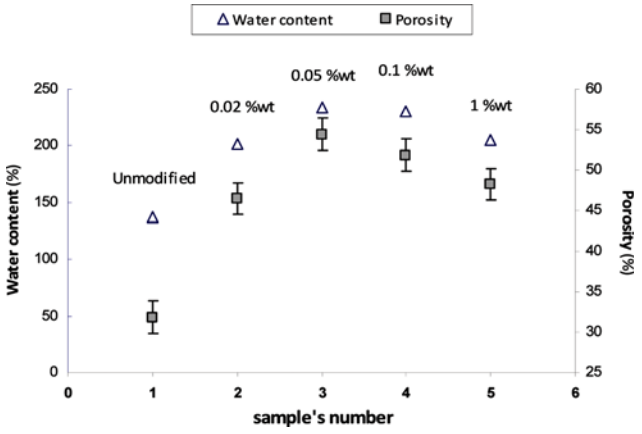

Fig. 7. The effect of titanium dioxide nanoparticles concentration on water content and porosity of prepared PES based membranes.

solvent and non-solvent during fabrication process, which declines the porosity of prepared membranes. Increase of casting solution viscosity by increase of nanoparticles concentration decreases the free spaces in the membrane matrix. In addition, the nanoparticle agglomeration at high NPs concentration decreases the water content and porosity.

5. Mechanical Strength of Prepared Membranes

The effect of nanoparticle content ratio on tensile stress behavior of prepared membranes was studied by Universal Testing Machine. Obtained results (Fig. 8) showed that mechanical stability of prepared membranes was improved by increase of nanoparticle content ratio up to 0.05 wt% in prepared membranes. This is due to

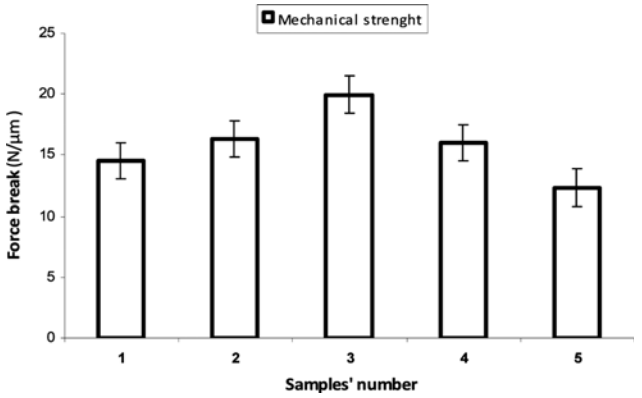

Fig. 8. The effect of nanoparticles concentration on mechanical strength behaviour of prepared membranes.

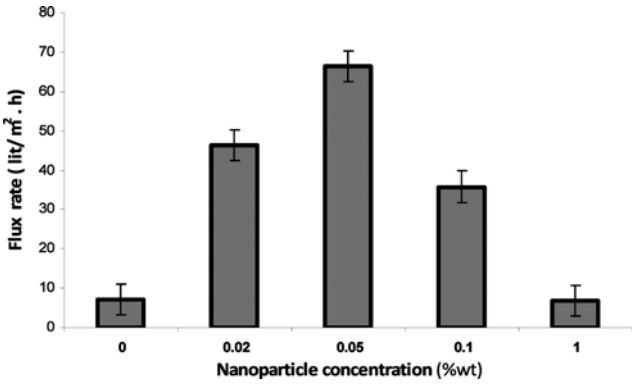

Fig. 9. The effect of titanium dioxide concentration in casting solution on membrane flux.

the presence of strong interfacial bonding between the polymers and nanoparticles, which improves mechanical property. Moreover, well dispersed nanoparticles make favorable molecular interactions between the nanoparticles and binder [24,35-38]. The membrane tensile stress was decreased again by more nanoparticle content ratio from 0.05 to 1 wt% due to discontinuity of polymer binder, which tends to form discrete phase.

6. Flux and Glycerol Rejection

The obtained results (Fig. 9) revealed that membrane flux was enhanced sharply by increase of TiO_2 nanoparticle concentration up to 0.05 wt% in the casting solution. This may be due to increase of membrane heterogeneity and membrane porosity by using TiO_2 NPs, which provides more space for fluid passage and improves the membrane flux. The membrane flux was decreased again by more increase of nanoparticle content ratio from 0.05 to 1 wt%. This can be explained with respect to NPs agglomeration and membrane channels blockage at high nanoparticle concentrations [39], which decreases the fluid flux. Moreover, decrease of membrane porosity at high nanoparticles concentration declines the flux.

The separation efficiency for prepared membranes as ratio of membrane performance to water washing performance is shown in Fig. 10.

Obtained results indicated that separation efficiency was enhanced sharply by increase of nanoparticle content ratio up to 0.05 wt%.

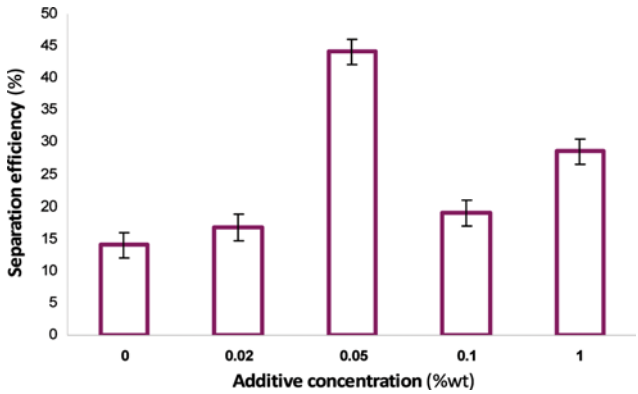

Fig. 10. The separation efficiency of prepared membranes with different percentages of titanium dioxide concentration.

Table 3. Comparison between the properties of purified biodiesel in this study and D6751 standard

Sample	Density (-)	Kinematic viscosity (mm^2/s)	Flash point (°C)
Biodiesel purified	0.88	4.91	107
ASTM D6751-Standard	0.88	Maximum 6	At least 93

This may be due to decrease of membrane roughness, which decreases the possibility of stagnant layer formation on membrane surface and improves the membrane rejection. Moreover, the antifouling property of TiO_2 nanoparticles improves the selectivity.

The separation efficiency declined again by more increase of nanoparticle concentration from 0.05 to 1 wt% in prepared membranes, which was due to increase of membrane surface roughness. Also, NPs accumulation at high nanoparticle content ratio reduced the separation efficiency.

The modified membranes containing titanium dioxide NPs showed better separation efficiency compared to pristine PES membrane. Among the prepared membranes, the modified membrane containing 0.05 wt% TiO_2 nanoparticles, with highest flux and separation efficiency and suitable physico-chemical characteristic showed more appropriate performance compared to others.

CONCLUSIONS

The purification of biodiesel produced from waste cooking oil was carried out by using PES-co-TiO_2 NPs nanocomposite membranes. Titanium dioxide nanoparticles were used as inorganic filler additive in membrane matrix. SEM images showed uniform NPs distribution on the surface and in the bulk of membrane matrix. Also, XRD results indicated a crystalline structure for the nanocomposite membranes. The membranes selectivity was also improved initially by increase of TiO_2 nanoparticles and then decreased. AFM results exhibited that membrane roughness was decreased sharply by increase of nanoparticle concentration in the casting solution. Results revealed that membrane flux was increased initially by increase of nanoparticle concentration up to 0.05 wt% in the casting solution and then decreased again by more increase in nanoparticles content ratio from 0.05 to 1 wt%. Furthermore, the mechanical stability of prepared membranes was improved by increase of nanoparticles concentration up to 0.05 wt% in prepared membranes. The membrane tensile stress was decreased again by further increase of nanoparticles concentration from 0.05 to 1 wt% due to discontinuity of polymer chain binder. Among the prepared membranes, modified membrane containing 0.05 wt% TiO_2 nanoparticles showed better performance compared to others. Also, a typical comparison between the properties of purified biodiesel in this study and D6751 standard according to the international legislation is given in Table 3.

REFERENCES

1. I. M. Atadashi, M. K. Aroua, A. R. Abdul Aziz and N. M. N. Sulaiman, *J. Membr. Sci.*, **422**, 154 (2012).
2. I. M. Atadashi, A. R. Abdul-Aziz and N. M. N. Sulaiman, *Renew. Sustain. Energy Rev.*, **16**, 3456 (2012).
3. I. M. Atadashi, M. K. Aroua, A. R. Abdul Aziz and N. M. N. Sulaiman, *Renew. Sustain. Energy Rev.,* **15**, 5051 (2011).
4. M. Jos Alves, S. M. Nascimento, I. G. Pereira, M. I. Martins, M. R. V. L. Cardoso and M. Reis, *Renewable Energy*, **58**, 15 (2013).
5. Y. Wang, X. Wang, Y. Liu, S. Ou, Y. Tan and S. Tang, *Fuel Process. Technol.*, **90**, 422 (2009).
6. J. Saleh, M. A. Dube and A. Y. Tremblay, *Fuel Process. Technol.*, **92**, 1305 (2011).
7. J. Saleh, A. Y. T. Marc and A. Dub, *Fuel Process. Technol.*, **89**, 2260 (2010).
8. M. R. Jakeria and A. S. M. A. Haseeb, *Renew. Sustain. Energy Rev.*, **30**, 154 (2014).
9. R. Othman, A. W. Mohammad, M. Ismail and J. Salimon, *J. Membr. Sci.*, **348**, 287 (2010).
10. M. Berrios, M. A. M., A. F. Chica and A. Martín, *Appl. Energy*, **88**, 3625 (2011).
11. H. Y. He, X. Gu and S. L. Zhu, T.U. Department of Chemical Engineering, Editor (2006).
12. S. Cheong, School of Mechanical and Aerospace Engineering (2009).
13. E. F. Aransiola, T. V. Ojumu, O. O. Oyekola and T. F. Madzimbamuto, *Biomass Bioenergy*, **61**, 276 (2014).
14. M. Peyravi, A. Rahimpour and M. Jahanshahi, *J. Membr. Sci.*, **473**, 72 (2015).
15. M. C. S. Gomes, N. C. Pereira and S. T. Davantel de Barros, *J. Membr. Sci.*, **352**, 271 (2010).
16. S. Roy, S. A. Ntim, S. Mitra and K. K. Sirkar, *J. Membr. Sci.*, **375**, 81 (2011).
17. F. T. Minhas, S. Memon, M. I. Bhanger, N. Iqbal and M. Mujahid, *Appl. Surf. Sci.*, **282**, 887 (2013).
18. P. Bondioli and L. Della Bella, *Eur. J. Lip. Sci. Technol.*, **107**, 153 (2005).
19. S. M. Hosseini, F. Jeddi, M. Nemati, S. S. Madaeni and A. R. Moghadassi, *Desalination*, **341**, 107 (2014).
20. X. Li, Z. Wang, H. Lu, C. Zhao, H. Na and C. Zhao, *J. Membr. Sci.*, **254**, 147 (2005).
21. S. M. Hosseini, S. S. Madaeni and A. R. Khodabakhshi, *Sep. Sci. Technol.*, **45**, 2308 (2010).
22. T. Sata, The Royal Society of Chemistry, Cambridge, United Kingdom (2004).
23. Y. Tanaka, Elsevier, Netherlands (2007).
24. G. Wu, S. Gan, L. Cui and Y. Xu, *Appl. Surf. Sci.*, **254**, 7080 (2008).
25. I. M. Wienk, R. M. Boom and M. A. M. Beerlage, *J. Membr. Sci.*, **113**, 361 (1996).
26. A. Sotto, A. Boromand, R. Zhang, P. Luis, J. M. Arsuag, J. Kim and B. Van der Bruggen, *J. Colloid Interface Sci.*, **363**, 540 (2011).
27. A. Rahimpour, M. Jahanshahi, S. Khalili, A. Mollahosseini, A. Zirepour and B. Rajaeian, *Desalination*, **286**, 99 (2012).
28. J. Feng Li, Z. L. Xu, H. Yang, L. Y. Yu and M. Liu, *Appl. Surf. Sci.*, **255**, 4725 (2009).
29. A. Rahimpour, M. Jahanshahi, B. Rajaeian and M. Rahimnejad, *Desalination*, **278**, 343 (2011).
30. F. Q. Wu, S. P. Ruan and X. P. Li, *J. Funct. Mater.*, **32**, 69 (2001).
31. Y. Yang, H. Zhang, P. Wang, Q. Zheng and J. Li, *J. Membr. Sci.*, **28**, 231 (2007).

32. A. Razmjou, J. Mansouri and V. Chen, *J. Membr. Sci.*, **378**, 73 (2011).
33. P. Daraei, S. S. Madaeni, N. Ghaemi, M. Khadivi, B. Astinchap and R. Moradian, *J. Membr. Sci.*, **444**, 184 (2013).
34. V. Vatanpour, S. S. Madaeni, R. Moradian, S. Zinadini and B. Astinchap, *Sep. Purif. Technol.*, **90**, 69 (2012).
35. A. Zendehnam, M. Rabieyan, S. M. Hosseini and S. Mokhtari, *Korean J. Chem. Eng.*, **32**(3), 501 (2015).
36. S. M. Hosseini, A. R. Hamidi, S. S. Madaeni and A. R. Moghadassi, *Korean J. Chem. Eng.*, **32**(3), 429 (2015).
37. S. M. Hosseini, P. Koranian, A. Gholami, S. S. Madaeni, A. R. Moghadassi, P. Sakinejad and A. R. Khodabakhshi, *Desalination*, **329**, 62 (2013).
38. S. M. Hosseini, S. S. Madaeni and A. R. Khodabakhshi, *J. Appl. Polym. Sci.*, **118**, 3371 (2010).
39. P. Daraei, S. S. Madaeni, N. Ghaemi, E. Salehi, M. A. Khadivi, R. Moradian and B. Astinchap, *J. Membr. Sci.*, **415**, 250 (2012).